

Multiple CD4⁺ T Cell Subsets Produce Immunomodulatory IL-10 During Respiratory Syncytial Virus Infection

Kayla A. Weiss,* Allison F. Christiaansen,[†] Ross B. Fulton,^{†,1} David K. Meyerholz,[‡] and Steven M. Varga*^{*,†,‡}

The host immune response is believed to contribute to the severity of pulmonary disease induced by acute respiratory syncytial virus (RSV) infection. Because RSV-induced pulmonary disease is associated with immunopathology, we evaluated the role of IL-10 in modulating the RSV-specific immune response. We found that IL-10 protein levels in the lung were increased following acute RSV infection, with maximum production corresponding to the peak of the virus-specific T cell response. The majority of IL-10-producing cells in the lung during acute RSV infection were CD4⁺ T cells. The IL-10-producing CD4⁺ T cells included Foxp3⁺ regulatory T cells, Foxp3⁻ CD4⁺ T cells that coproduce IFN- γ , and Foxp3⁻ CD4⁺ T cells that do not coproduce IFN- γ . RSV infection of IL-10-deficient mice resulted in more severe disease, as measured by increased weight loss and airway resistance, as compared with control mice. We also observed an increase in the magnitude of the RSV-induced CD8⁺ and CD4⁺ T cell response that correlated with increased disease severity in the absence of IL-10 or following IL-10R blockade. Interestingly, IL-10R blockade during acute RSV infection altered CD4⁺ T cell subset distribution, resulting in a significant increase in IL-17A-producing CD4⁺ T cells and a concomitant decrease in Foxp3⁺ regulatory T cells. These results demonstrate that IL-10 plays a critical role in modulating the adaptive immune response to RSV by limiting T-cell-mediated pulmonary inflammation and injury. *The Journal of Immunology*, 2011, 187: 3145–3154.

The lung environment, with its constant exposure to inert foreign Ags, must preserve a fine balance between tolerance and inflammation to effectively clear respiratory pathogens while, at the same time, maintaining tissue homeostasis. Improper regulation of a pathogen-induced immune response can result in excessive immune-mediated injury to the lung tissue, termed immunopathology. Respiratory syncytial virus (RSV) is a leading cause of lower respiratory tract infections in young children, the elderly, and immunocompromised individuals (1–6). The host immune response is thought to contribute to the severity of RSV-induced respiratory disease (7). In addition to RSV, other respiratory viral pathogens, such as pandemic influenza strains and human coronaviruses that cause severe acute respiratory

syndrome (SARS), are believed to induce a poorly regulated immune response resulting in immune-mediated disease (8, 9).

The lung environment contains a number of mechanisms that regulate the immune response (10), including the production of immunosuppressive cytokines such as IL-10. Both innate and adaptive immune cells have the capacity to produce IL-10, including mast cells, NK cells, neutrophils, eosinophils, macrophages, dendritic cells (DCs), CD4⁺ T cells, CD8⁺ T cells, and B cells (11). In addition, almost all immune cells express the IL-10R1 and IL-10R2 subunits (12–14), which together compose the IL-10 receptor (IL-10R), and are thus capable of responding to IL-10. Due to the broad expression of IL-10 and the potential responsiveness of most immune cells, it is clear that IL-10 can influence both innate and adaptive immunity.

IL-10 mediates pleiotropic effects on the immune response, including suppressing the activation and/or effector functions of immune cells. In macrophages, IL-10-induced signaling results in reduced production of proinflammatory cytokines and chemoattractants required for the recruitment of T cells, monocytes, DCs, and neutrophils to the site of infection (15). In addition, IL-10 suppresses the surface expression of MHC class II and costimulatory molecules on macrophages and immature DCs, resulting in the decreased activation and proliferation of T cells (16–18). IL-10 can also directly inhibit T cell cytokine production (e.g., IL-2, IL-5, and TNF) and induce T cell anergy (19–21).

The critical role of IL-10 during persistent infections has been well established (15, 22); however, its capacity to modulate the immune response during an acute viral infection resulting in immunopathology remains unknown. In the murine RSV infection model, it is evident that RSV-induced disease is immune mediated because depletion of T cells ameliorates disease even in the presence of prolonged viral replication (23, 24). This makes RSV an ideal model for studying dysregulation of an immune response in the lung mucosal environment. To dissect the role of IL-10

*Interdisciplinary Graduate Program in Immunology, University of Iowa, Iowa City, IA 52242; [†]Department of Microbiology, University of Iowa, Iowa City, IA 52242; and [‡]Department of Pathology, University of Iowa, Iowa City, IA 52242

¹Current address: Department of Laboratory Medicine and Pathology, Center for Immunology, University of Minnesota Medical Center, Minneapolis, MN.

Received for publication March 16, 2011. Accepted for publication July 17, 2011.

This work was supported by National Institutes of Health Grant R01 AI063520 (to S.M.V.) and Training in Statistics in Microbiology, Infectious Diseases, and Bioinformatics Training Grant T32 GM077973 (to K.A.W.). The multiplex cytokine assay data presented were obtained at the Flow Cytometry Facility, which is a Carver College of Medicine Core Research Facilities/Holden Comprehensive Cancer Center Core Laboratory at the University of Iowa. The facility is funded through user fees and the generous financial support of the Carver College of Medicine, Holden Comprehensive Cancer Center, and Iowa City Veteran's Administration Medical Center.

Address correspondence and reprint requests to Dr. Steven Varga, Department of Microbiology, University of Iowa, 51 Newton Road, 3-532 B.S.B., Iowa City, IA 52242. E-mail address: steven-varga@uiowa.edu

The online version of this article contains supplemental material.

Abbreviations used in this article: BAL, bronchoalveolar lavage; DC, dendritic cell; IAV, influenza A virus; ID, interstitial disease; KO, knockout; medLN, mediastinal lymph node; PAS, periodic acid-Schiff; Penh, parameter-enhanced pause; p.i., post-infection; PVA, perivascular aggregate of leukocytes; RSV, respiratory syncytial virus; SARS, severe acute respiratory syndrome; Treg, T regulatory cell.

Copyright © 2011 by The American Association of Immunologists, Inc. 0022-1767/11/\$16.00

during a respiratory viral infection resulting in immunopathology, we first identified the IL-10-producing cells during acute RSV infection and examined the effects of IL-10 deficiency on the adaptive immune response. We demonstrate that CD4⁺ T cells account for the majority of IL-10 production during the peak of the virus-specific T cell response. Furthermore, we show that multiple CD4⁺ T cell subsets produce IL-10. In the absence of IL-10 or following IL-10R blockade, we observed a significant increase in RSV-induced disease severity correlating with the kinetics of the RSV-specific adaptive immune response. Finally, we show that IL-10R blockade results in an increase in the number of Th1 and Th17 cells with a concomitant decrease in the number of T regulatory cells (Tregs). Taken together, our data suggest that IL-10 plays a critical role in modulating the adaptive immune response to acute RSV infection and in preventing immune-mediated pulmonary injury.

Materials and Methods

Mice, infection, and Ab treatment

Female BALB/cAnNCr mice 6–8 wk old were purchased from the National Cancer Institute (Frederick, MD). BALB/c IL-10-deficient mice (IL-10 knockout [KO]) were obtained from Dr. Daniel Berg (University of Iowa, Iowa City, IA) (25, 26). VERT-x mice, expressing an IL-10-eGFP reporter, were obtained from Dr. Christopher Karp (Cincinnati Children's Hospital Research Foundation and University of Cincinnati College of Medicine, Cincinnati, OH) (27). The A2 strain of RSV was a gift from Dr. Barney Graham (National Institutes of Health, Bethesda, MD) and was propagated on HEP-2 cells (American Type Culture Collections, Manassas, VA). For infections, mice were anesthetized with isoflurane and infected intranasally with $1-3 \times 10^6$ PFU of RSV. In some experiments, mice were administered either 0.5 mg rat IgG (MP Biomedicals, Aurora, OH) or 0.5 mg anti-IL-10R mAb (clone 1B1.3) via i.p. injections starting 1 d prior to infection and every other day thereafter. CD4⁺ and/or CD8⁺ T cells were depleted via i.p. injection of 0.25 mg of anti-CD4 (clone GK1.5) and/or anti-CD8 (clone 2.43) Ab at days -2 and +2 relative to infection. All experimental procedures involving mice were approved by the University of Iowa Animal Care and Use Committee.

Disease measurements

Disease was assessed daily by monitoring weight loss as well as pulmonary function using an unrestrained whole-body plethysmograph (Buxco Electronics, Wilmington, NC), as previously described (28, 29). Pressure and volume differences in the chamber caused by respiration were monitored for 5 min and recorded to obtain a daily average to calculate the dimensionless parameter-enhanced pause (Penh), as previously described (30). Penh positively correlates to airway hyperreactivity (30), which is narrowing of the small airways in response to stimuli.

Tissue processing

Lungs and bronchoalveolar lavage (BAL) fluid from mice were harvested as previously described (31). Lung tissue and lymph nodes were digested in 4 ml or 1 ml, respectively, of HBSS with CaCl₂ and MgCl₂ (Life Technologies, Grand Island, NY) supplemented with 60 U/ml DNase I (Sigma-Aldrich, St. Louis, MO) and 125 U/ml collagenase (Invitrogen, Carlsbad, CA) for 30 min at 37°C. After digestion, lungs were pressed through a wire mesh screen (Collector; Bellco Glass, Vineland, NJ) to create a single-cell suspension. Mediastinal lymph nodes (medLNs) were disrupted by gentle pressing between the ends of frosted glass slides (Surgipath, Richmond, IL).

Extracellular staining

A total of $1-2 \times 10^6$ cells were placed in a 96-well round-bottom plate (Corning, Corning, NY). Cells were incubated with mAbs for extracellular proteins—CD90.2 (Thy1.2; clone 53-2.1), CD4 (clone RM4.5), CD8 (clone 53-6.7), CD11a (clone M17/4), and CD44 (clone IM7)—and simultaneously blocked with anti-FcγRII/III mAb (clone 93) (all mAbs obtained from eBioscience, San Diego, CA) in FACS buffer (PBS, 2% FCS, 0.02% sodium azide) for 30 min at 4°C. Cells were subsequently washed three times with FACS buffer at 4°C, fixed with FACS lysing solution (BD Biosciences, San Diego, CA) for 15 min at room temperature, washed three times with FACS buffer at 4°C and resuspended in FACS

buffer for analysis. Samples were collected on a BD FACSCanto flow cytometer and data were analyzed using FlowJo software (Tree Star, Ashland, OR).

Ex vivo cell stimulations

Cells were incubated at $1-2 \times 10^6$ cells/well in a 96-well round-bottom plate (Corning). For peptide stimulations, cells were incubated with or without 1 μM M2₈₂₋₉₀ peptide (Biosynthesis, Lewisville, TX) and 10 μg/ml brefeldin A (Sigma-Aldrich) in RPMI 1640 supplemented with 10% FCS (Atlanta Biologicals, Lawrenceville, GA), 5 nM 2-ME (Sigma), 2 mM L-glutamine, 10 U/ml penicillin, 10 μg/ml streptomycin sulfate, 10 mM HEPES, 1 mM sodium pyruvate, and 0.1 mM MEM nonessential amino acids (all obtained from Life Technologies) for 5 h at 37°C (31). Alternatively, cells were stimulated in the presence or absence of 50 ng/ml PMA (Sigma-Aldrich), and 500 ng/ml ionomycin (Sigma-Aldrich) in the presence of 10 μg/ml brefeldin A in 10% FCS complemented RPMI 1640 for 5 h at 37°C.

Intracellular cytokine staining

Briefly after ex vivo stimulation, cells were stained for extracellular proteins and fixed in FACS lysing solution as described above. Cells were subsequently incubated in FACS buffer containing 0.5% saponin (Sigma-Aldrich) and intracellular cytokine Abs—IL-10 (clone JES5-16E3), IFN-γ (clone XMG1.2), TNF-α (clone MP6-XT22), IL-17A (clone TC11-18H10.1) (all mAbs obtained from eBioscience)—for 30 min at 4°C. Cells were washed twice with FACS buffer containing saponin, once with FACS buffer, and resuspended in FACS buffer prior to analysis on a BD FACSCanto.

Foxp3 staining

After staining extracellular proteins as described above, cells were stained for Foxp3, using the Mouse Regulatory T Cell Staining Buffer Kit (eBioscience) according to the manufacturer's instructions. Cells were stained with mAbs against Foxp3 (clone FJK-16s), Helios (clone 22F6), IL-10 (clone JES5-16E3), and IFN-γ (clone XMG1.2) (all mAbs obtained from eBioscience). After staining, cells were resuspended in FACS buffer prior to analysis.

Plaque assays

Lungs were harvested on days 4 and 7 postinfection (p.i.) and processed for plaque assays as previously described (32).

ELISAs

Lungs from RSV-infected mice were disrupted using a tissue homogenizer (Ultra-Turrax T25; IKA Works, Wilmington, NC) in RPMI 1640 containing 10% FCS and a 1/200 dilution of a protease inhibitor mixture (Sigma). Lung homogenates were centrifuged at 2000 rpm for 10 min. Cytokine protein levels in the supernatant were determined for IL-10 and IFN-γ by ELISA, as previously described (33) (IL-10 and IFN-γ Abs were obtained from eBioscience). Detection limits for cytokine protein levels were 62.5 pg/ml for IL-10 and 1250 pg/ml for IFN-γ.

Multiplex bead assays

Lungs from RSV-infected IL-10 KO and wild-type mice were harvested and supernatants were collected as described above. A Milliplex kit was used to determine the protein levels of 27 different cytokines and chemokines by following the manufacturer's instructions (Millipore, Billerica, MA). The assay was run on a BioPlex instrument (Bio-Rad, Hercules, CA).

Histological examination

Whole lungs from naive and RSV-infected rIgG and anti-IL-10R mAb-treated mice on day 6 p.i. were fixed in 10% formalin (Thermo Fisher Scientific, Waltham, MA). Fixed lungs were embedded in paraffin, sectioned at 4-μm thickness, and stained by the University of Iowa Comparative Pathology Laboratory. Slides were stained with either H&E or periodic acid-Schiff (PAS) and randomized and blinded for analysis by a board-certified veterinary pathologist (Dr. D. Meyerholz, University of Iowa). Sectioned slides were scored for perivascular aggregates of leukocytes (PVA; 1, within normal parameters; 2, small numbers of solitary cells with uncommon aggregates; 3, multifocal small to moderate aggregates; and 4, moderate to high cellularity with multifocal large cellular aggregates that may be expansive into adjacent tissues), interstitial disease (ID; 1, within normal parameters; 2, mild, detectable focal to multifocal

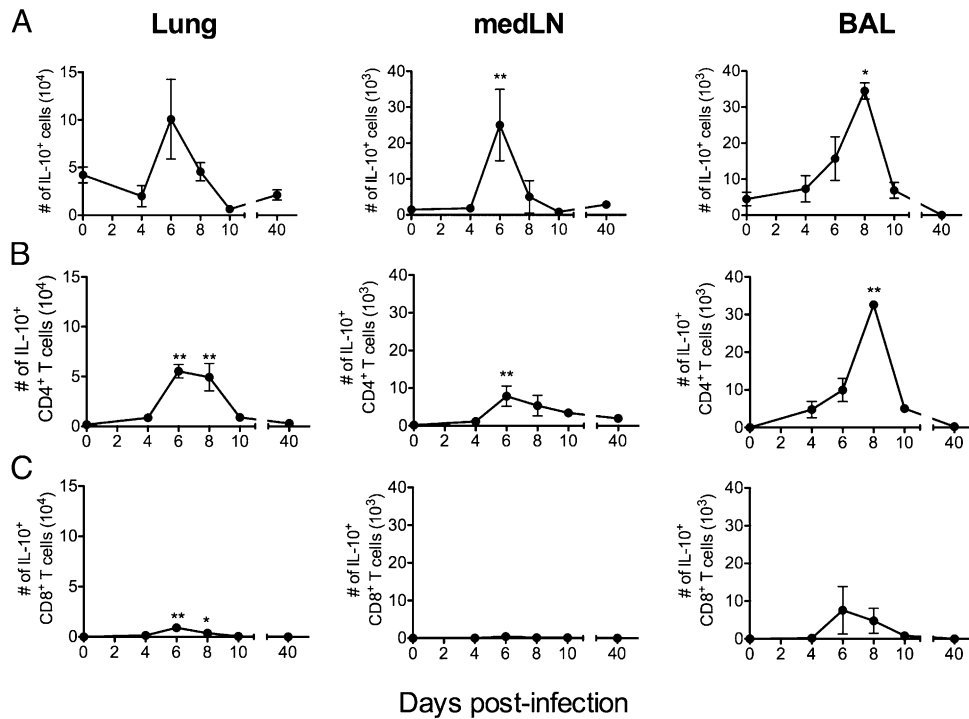


FIGURE 1. The kinetics of IL-10–producing cells during acute RSV infection. At the indicated time points, cells from the lung, medLNs, and BAL of RSV-infected mice were isolated and stimulated with PMA and ionomycin, followed by intracellular cytokine staining for IL-10. The total number of IL-10⁺ cells (A), IL-10⁺ CD4⁺ T cells (B), and IL-10⁺ CD8⁺ T cells (C) in the lung, medLNs, and BAL. To determine statistical significance, an ANOVA was performed with a Dunnett’s post test making comparisons between each time point (days 4, 6, 8, and 10) and baseline (day 0). Cumulative data from two independent experiments are shown (*n* = 8). **p* < 0.05, ***p* < 0.01.

congestion, with uncommon to small numbers of leukocytes and some atelectasis; 3, moderate, multifocal to coalescing congestion, leukocyte cellularity, and atelectasis, with rare luminal leakage of cellular and fluid debris; and 4, severe, coalescing interstitial congestion, leukocytes, and atelectasis, with admixed extensive loss of airspace and luminal accumulation of cellular and fluid debris), edema (1, none; 2, rare, with alveoli with wispy to partial pools of eosinophilic seroproteinaceous fluid; 3, focal microscopic fields with contiguous alveoli partially filled by pools of fluid; and 4, multiple fields having coalescing alveoli filled by pools of fluid), and mucus (1, none; 2, epithelial mucinous hyperplasia with none to rare luminal mucus; 3, epithelial mucinous hyperplasia with luminal mucus accumulation in airways; and 4, severe mucinous change with some airways completely obstructed by mucus). The total score is the sum of the PVA, ID, edema, and mucus scores.

Statistical analysis

Data were graphically compiled using Prism software (Graphpad Software, San Diego, CA), with bars representing the SEM. Statistical analysis was completed using InStat software (Graphpad Software); unpaired, two-tailed Student *t* tests and ANOVAs with a Dunnett’s post test were calculated to determine statistical significance at a level of α = 0.05.

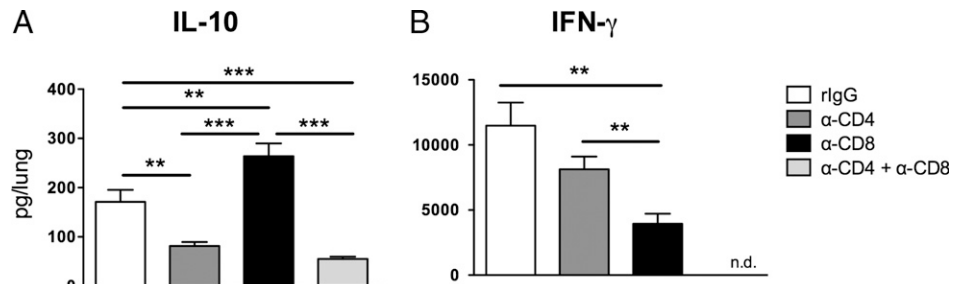
Results

CD4⁺ T cells account for the majority of IL-10–producing cells during the peak of the virus-specific T cell response

To determine the role of IL-10 during acute RSV infection, we first examined the kinetics and cellular source of IL-10 production. Cells from the lung, medLNs, and lung airways (i.e., BAL) were stimulated in vitro with PMA and ionomycin and stained for intracellular IL-10. The total number of IL-10–producing cells peaked on day 6 p.i. in the lung and medLNs and on day 8 p.i. in the BAL (Fig. 1A). CD4⁺ T cells constituted the majority of IL-10–producing cells (Fig. 1B). In contrast, IL-10–producing CD8⁺ T cells did not accumulate in large numbers in any of the tissues analyzed (Fig. 1C).

To verify our results that were obtained with in vitro stimulation, we used mice that express an IL-10–eGFP reporter to examine IL-10–producing cells directly ex vivo during an acute RSV infection. In agreement with our in vitro restimulation data discussed above, the frequency of IL-10–eGFP⁺ cells peaked on day 8 p.i. in the lung and BAL (Supplemental Fig. 1). Approximately 80–90% of

FIGURE 2. CD4⁺ T cells are the primary in vivo source of IL-10 during acute RSV infection. Wild-type mice were treated with depleting anti-CD4 and/or anti-CD8 mAbs or control rat IgG and subsequently infected with RSV. On day 6 p.i., lungs were analyzed for IL-10 (A) and IFN- γ protein (B) via ELISA. Cumulative data from two independent experiments are shown (*n* = 8). **p* < 0.05, ***p* < 0.01, ****p* < 0.001. n.d., none detected.



IL-10-eGFP⁺ cells on days 6 and 8 p.i. were T cells, as identified by Thy1.2 staining in the lung and BAL (Supplemental Fig. 1). Within the Thy1.2⁺ population, CD4⁺ T cells represented the majority of IL-10-eGFP⁺ T cells in lungs and BAL at all time points examined. Taken together, these data demonstrate that CD4⁺ T cells account for the majority of IL-10-producing cells during the peak of the virus-specific T cell response.

To confirm that CD4⁺ T cells produce the majority of IL-10 in vivo during RSV infection, we quantified IL-10 protein levels in the lungs of mice depleted of CD4⁺ and/or CD8⁺ T cells. Our results indicate that CD4⁺ T cells were responsible for the majority of IL-10 protein produced in the lung during an acute RSV infection (Fig. 2A). Elimination of CD8⁺ T cells resulted in increased IL-10 production, suggesting that CD8⁺ T cells may suppress IL-10 production by CD4⁺ T cells. IFN- γ production was also measured using the above approach, and, as expected, CD8⁺ T cells produced significantly more IFN- γ than did the CD4⁺ T cells in response to RSV infection (Fig. 2B). Taken together, these data demonstrate that CD4⁺ T cells are the major producers of IL-10 in vivo during an acute RSV infection. The capacity of CD4⁺ T cells to produce IL-10 suggests their potential to significantly modulate the immune response via anti-inflammatory cytokine production.

Multiple CD4⁺ T cell subsets produce IL-10 in response to RSV infection

Because CD4⁺ T cells accounted for the majority of RSV-induced IL-10-producing cells, we next determined the CD4⁺ T cell subsets responsible for the IL-10 production. On day 6 p.i., lung, medLN, and BAL cells were stimulated in vitro with PMA and ionomycin and stained for intracellular IL-10, IFN- γ , and Foxp3. In all tissues analyzed, we observed equal proportions of IL-10⁺ CD4⁺ T cells that produced only IL-10, coproduced IFN- γ (i.e., Th1 cells), or coexpressed Foxp3 (i.e., Tregs) (Fig. 3). Interestingly, in the BAL we observed a small population of Foxp3⁺ Tregs that coproduced IL-10 and IFN- γ . These data demonstrate that multiple CD4⁺ T cell subsets contribute to IL-10 production during an acute RSV infection.

In addition, we determined the frequency of IL-10-producing cells within these CD4⁺ T cell subsets (Table I). On day 6 p.i., we

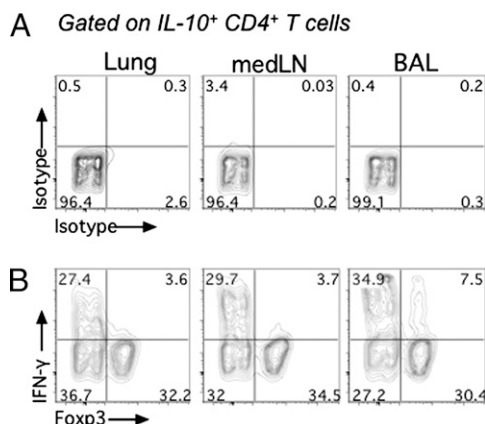


FIGURE 3. Multiple CD4⁺ T cell subsets produce IL-10 during acute RSV infection. At day 6 p.i., cells from the lung, medLNs, and BAL were stimulated with PMA and ionomycin. Cells were subsequently stained for CD4, Thy1.2, IL-10, Foxp3, and IFN- γ . Gated IL-10⁺ CD4⁺ T cells depicting isotype control staining (A) or Foxp3 expression (x-axis) and IFN- γ production (y-axis) (B) are shown. Plots are concatenated using Flowjo software from one of two independent experiments displaying equal representation from four individual mice ($n = 4$).

Table I. Frequencies of cytokine-producing CD4⁺ T cells on day 6 following RSV infection

CD4 ⁺ T cell	IFN- γ ⁺ IL-10 ⁻	IFN- γ ⁺ IL-10 ⁺	IFN- γ ⁻ IL-10 ⁺
Conventional (Foxp3 ⁻)			
Lung	10.1 \pm 3.2 ^a	2.8 \pm 0.9	2.5 \pm 0.4
MedLN	5.4 \pm 0.9	0.6 \pm 0.2	0.5 \pm 0.2
BAL	26.9 \pm 6.2	11.1 \pm 4.4	5.1 \pm 1.6
Regulatory (Foxp3 ⁺)			
Lung	1.6 \pm 1.6	2.0 \pm 1.7	15.9 \pm 1.4
MedLN	1.9 \pm 1.0	0.6 \pm 0.2	6.5 \pm 1.1
BAL	3.1 \pm 2.6	8.8 \pm 4.1	36.7 \pm 6.0

^aPercent \pm SD.

observed the highest frequency of IL-10-only producing conventional and regulatory CD4⁺ T cells (5.1 \pm 1.6 and 36.7 \pm 6.0%, respectively) in the BAL. Furthermore, in the BAL we observed the highest proportion of conventional and regulatory CD4⁺ T cells that coproduce IL-10 and IFN- γ (11.1 \pm 4.4 and 8.8 \pm 4.1%, respectively) when compared with other tissues. In all tissues analyzed, IL-10-producing conventional and regulatory CD4⁺ T cells were observed as summarized in Table I. These data demonstrate the distribution of IL-10-producing cells in the conventional and regulatory CD4⁺ T cell compartments following acute RSV infection.

Increased RSV disease severity in the absence of IL-10 or following IL-10R blockade

To examine the role of IL-10 during acute RSV infection, we used either IL-10-deficient (IL-10 KO) mice or anti-IL-10R mAb to determine disease severity in the absence of IL-10 or following IL-10R blockade. IL-10 KO mice, compared with control mice, exhibited greater weight loss and increased Penh following acute RSV infection (Fig. 4A). Similar results were obtained from mice treated with anti-IL-10R mAb prior to and during RSV infection, compared with IgG-treated controls (Fig. 4B). These data indicate that IL-10 plays a critical role in limiting disease severity at the peak of the adaptive immune response during RSV infection.

To determine if IL-10 had an effect on viral titers, we performed plaque assays using whole lung homogenates to measure viral load at the peak of RSV replication (i.e., day 4 p.i.) and following viral clearance (i.e., day 7 p.i.). No significant differences were noted in viral titer at either time point in IL-10 KO mice (Fig. 5A) or anti-IL-10R mAb-treated mice (Fig. 5B). These results show that the effect of IL-10 deficiency on disease severity is not due to either

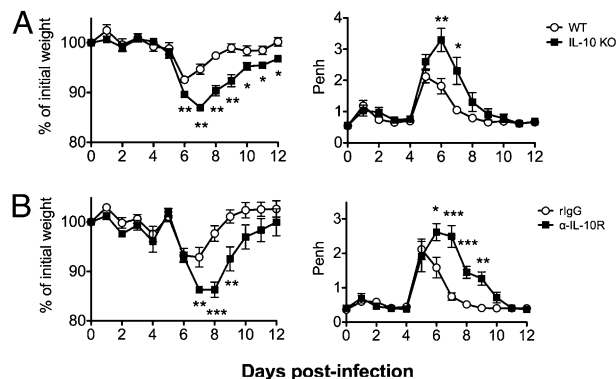


FIGURE 4. IL-10 influences RSV-induced disease severity. Weight loss depicted as the percent of initial weight and airway function (Penh) were assessed daily following RSV infection of IL-10-deficient (A) or anti-IL-10R mAb-treated mice (B). Cumulative data from two independent experiments are shown ($n = 8$). * $p < 0.05$, ** $p < 0.01$, *** $p < 0.001$.

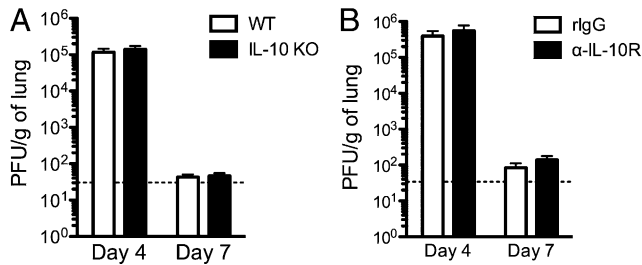


FIGURE 5. IL-10 does not affect RSV replication and clearance kinetics. Lungs were harvested on days 4 and 7 p.i. from RSV-infected IL-10 KO (A) or anti-IL-10R mAb treated mice (B). RSV titers were determined by plaque assay. The limit of detection is indicated as a horizontal dotted line. Cumulative data from two independent experiments are shown ($n = 8$).

altered viral replication or delayed viral clearance but instead may be the result of alterations of the RSV-specific immune response.

Increased inflammatory environment in the absence of IL-10

Given the increased disease severity observed during RSV infection in the absence of IL-10, we next examined the overall inflammatory environment in the lung following acute RSV infection. Using a multiplex bead assay, we quantified cytokine and chemokine protein levels from whole-lung homogenates at days 0, 4, 6, 8, and 10 p.i. from control and IL-10 KO mice infected with RSV. In the absence of IL-10, we observed a marked increase in the levels of proinflammatory cytokines and chemokines following RSV infection (Fig. 6). In the lungs of RSV-infected IL-10 KO mice, we observed a significant increase in IL-6 ($p < 0.01$) and TNF- α ($p < 0.001$) on day 6 p.i., and a significant increase in IFN- γ on days 6 ($p < 0.001$) and 8 p.i. ($p < 0.05$) as compared with control mice. In addition, CXCL1 was significantly increased in the lungs of IL-10 KO mice at days 4 ($p < 0.05$) and 6 p.i. ($p < 0.01$) and slightly increased on day 8 p.i., when compared with control mice. CXCL9 was increased and CCL2 was significantly increased ($p <$

0.001) on day 6 p.i. in the absence of IL-10 following RSV infection. Overall, in the absence of IL-10, we observed increased levels of proinflammatory cytokines and chemokines that can enhance inflammation and the infiltration of immune cells responsible for mediating immunopathology. Taken together, these data support the hypothesis that IL-10 plays a critical role in regulating the severity of RSV-induced pulmonary disease by regulating inflammation and limiting immunopathology.

IL-10R blockade results in an increase in the magnitude of the RSV-specific CD8⁺ T cell response

Because the increase in RSV-induced disease severity (days 6–8 p.i.) in the absence of IL-10 or following IL-10R blockade occurred during the rise of the RSV-specific adaptive immune response, we next investigated the impact of IL-10 deficiency on the magnitude of the RSV-specific CD8⁺ T cell response. In mice treated with anti-IL-10R mAb, the total number of CD8⁺ T cells significantly increased ($p < 0.01$) in the medLNs on day 6 p.i. (Fig. 7A). Furthermore, the total number of CD11a^{hi} CD8^{lo} T cells significantly increased ($p < 0.001$) in the medLNs of mice treated with anti-IL-10R mAb on day 6 p.i. (Fig. 7B), indicating the presence of Ag-experienced cells (34).

Using the M2₈₂₋₉₀ peptide to stimulate RSV-specific CD8⁺ T cells ex vivo, we observed a significant increase in the magnitude of the M2₈₂₋₉₀ RSV-specific CD8⁺ T cell response in the medLNs at day 6 p.i. ($p < 0.001$) and in the lung on day 8 p.i. ($p < 0.01$) (Fig. 7C, 7D). In the medLNs of mice treated with anti-IL-10R, we observed a significant increase in the total number of M2₈₂₋₉₀-specific CD8⁺ T cells producing IFN- γ ($p < 0.01$) or coproducing IFN- γ and TNF- α ($p < 0.0001$) on day 6 p.i. In the lungs of anti-IL-10R mAb-treated mice, there was a significant increase in the total number of M2₈₂₋₉₀-specific CD8⁺ T cells that produce IFN- γ ($p < 0.001$) or coproduce IFN- γ and TNF- α ($p < 0.01$) on day 8 p.i. These data indicate an increase in both the magnitude and the effector function of RSV-specific

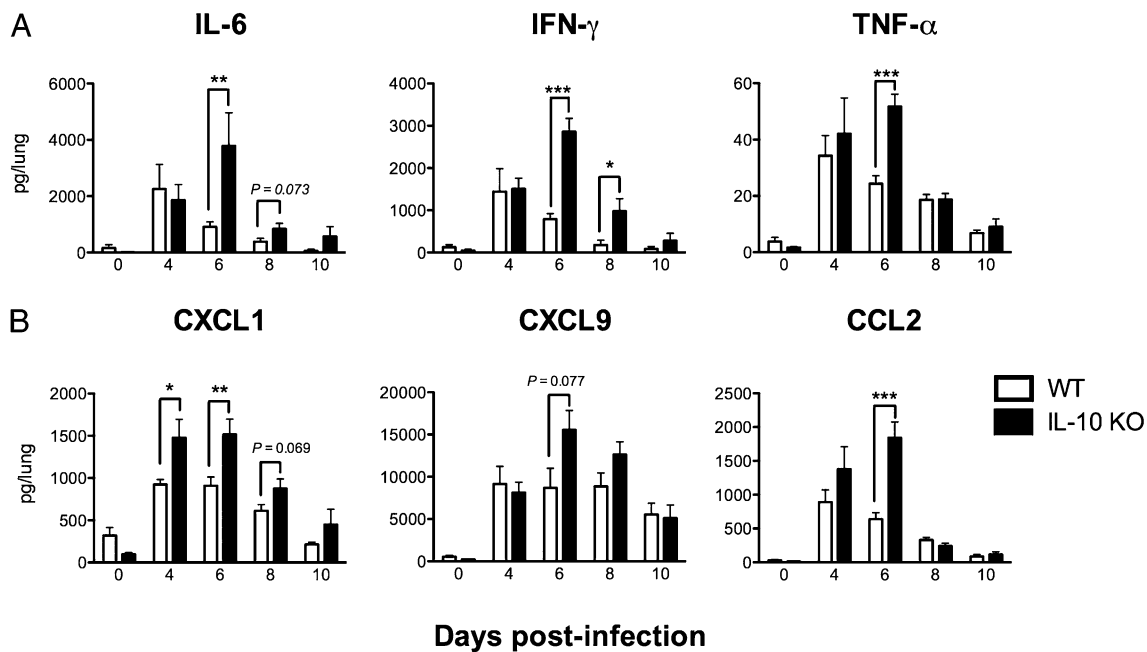


FIGURE 6. Increase in proinflammatory cytokines and chemokines in the absence of IL-10. At days 0, 4, 6, 8, and 10 p.i., lungs from IL-10 KO mice were harvested, and cytokine and chemokine protein levels within the lung supernatants were determined by multiplex cytokine array analysis. Proinflammatory cytokine (A) and chemokine (B) amounts in the lung. Cumulative data from two independent experiments are shown ($n = 8$). * $p < 0.05$, ** $p < 0.01$, *** $p < 0.001$.

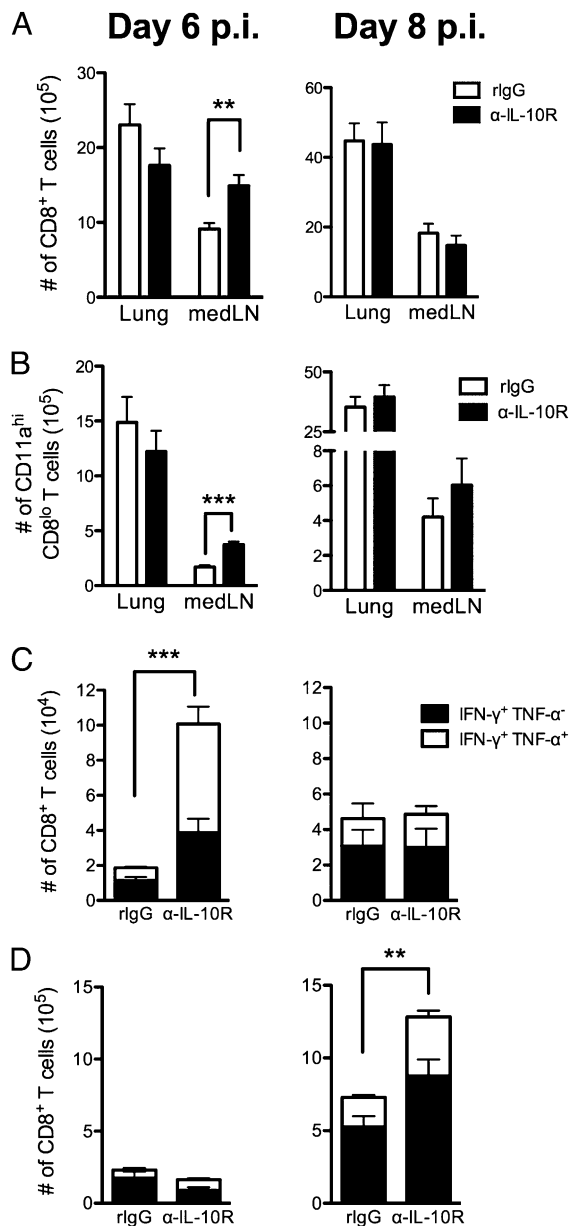


FIGURE 7. The magnitude of the CD8⁺ T cell response is increased following IL-10R blockade. Mice were treated with anti-IL-10R mAb, as described in *Materials and Methods*. *A*, The total number of CD8⁺ T cells at day 6 (*left*) and day 8 (*right*) p.i. in the lung and medLNs. *B*, The total number of CD11a^{hi} CD8⁺ T cells at day 6 (*left*) and day 8 (*right*) p.i. in the lung and medLNs. *C*, The total number of M2₈₂₋₉₀-specific CD8⁺ T cells producing only IFN-γ (closed bars) or coproducing IFN-γ and TNF-α (open bars) in the medLNs at day 6 (*left*) and day 8 (*right*) p.i. *D*, The total number of M2₈₂₋₉₀-specific CD8⁺ T cells producing only IFN-γ (closed bars) or coproducing IFN-γ and TNF-α (open bars) in the lung at day 6 (*left*) and day 8 (*right*) p.i. Data in *C* and *D* are displayed as stacked bar graphs, and the significant difference is marked for total responding cells. Cumulative data from two independent experiments are shown ($n = 8$). Unpaired, two-tailed Student *t* tests were used to compare groups. * $p < 0.05$, ** $p < 0.01$, *** $p < 0.001$.

CD8⁺ T cells following IL-10R blockade, demonstrating a role for IL-10 in limiting the RSV-specific CD8⁺ T cell response.

IL-10R blockade results in an increased Th1 CD4⁺ T cell response following acute RSV infection

Because the RSV-specific CD8⁺ T cell response was increased following IL-10R blockade, we next evaluated the impact of IL-

10 on the magnitude of the effector CD4⁺ T cell response during acute RSV infection. IL-10R blockade resulted in a significant increase in the total number of CD4⁺ T cells in the lung ($p < 0.01$) and BAL ($p < 0.05$) on day 8 p.i. (Fig. 8A). Intracellular cytokine staining for IFN-γ and TNF-α production by CD4⁺ T cells from the lung and medLNs stimulated with PMA and ionomycin revealed a significant increase ($p < 0.01$) in the total number of effector CD4⁺ T cells in the lung on day 8 p.i. in mice administered anti-IL-10R mAb (Fig. 8B). Furthermore, on day 8 p.i. in the lung, mice treated with anti-IL-10R mAb exhibited a significant increase in the number of CD4⁺ T cells that produce IFN-γ ($p < 0.001$) or coproduce IFN-γ and TNF-α ($p < 0.05$). Thus, similar to the increase in the number of CD8⁺ T cells described above, we observed an increase in the magnitude of the Th1 CD4⁺ T cell response in the lungs of mice administered anti-IL-10R mAb during acute RSV infection. This increase in the number of virus-specific IFN-γ-producing CD8⁺ and CD4⁺ T cells following IL-10R blockade during a RSV infection suggests a critical role for IL-10 in limiting the magnitude of the RSV-specific adaptive immune response.

Increased lung pathology following IL-10R blockade

To determine if the increased disease severity and effector CD8⁺ and CD4⁺ T cell response result in increased lung pathology following IL-10R blockade, histological analysis of sections from whole lungs were stained with either H&E or PAS and analyzed. On day 6 p.i., a significant increase ($p < 0.001$) was observed in lung pathology when scoring the PVA, ID, eosinophilic seroproteinaceous fluid in the airspaces (edema), and luminal mucus accumulation in the airways (Fig. 9A). The histology of rlgG-treated mice following RSV infection revealed tissue inflammation with minimal mucus in the luminal space of the lung airways (Fig. 9B). The histological sections from mice treated with anti-IL-10R mAb demonstrate the increased pathology with increased areas of edema, tissue inflammation, and increased mucus in the luminal space of the lung airways (Fig. 9C). Together these data indicate that IL-10R blockade results in increased lung pathology that is

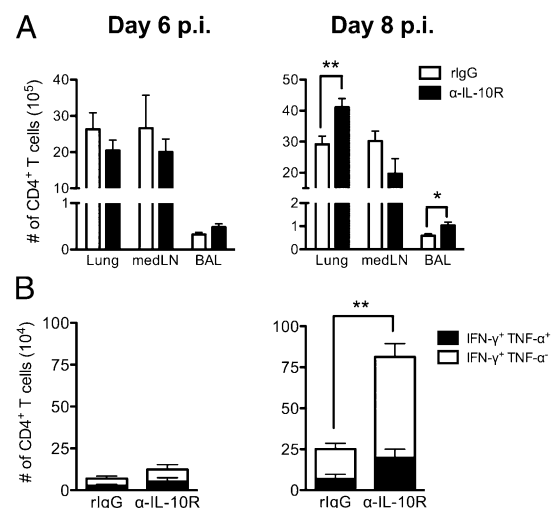


FIGURE 8. Increased Th1 response following IL-10R blockade. *A*, The total number of CD4⁺ T cells in the lung, medLNs, and BAL at day 6 (*left*) and day 8 (*right*) p.i. *B*, The total number of PMA- and ionomycin-stimulated CD4⁺ T cells producing only IFN-γ (closed bars) or coproducing IFN-γ and TNF-α (open bars) in the lung at day 6 (*left*) and day 8 (*right*) p.i. Data are displayed as stacked bar graphs, and the significant difference is marked for total responding cells. Cumulative data from two independent experiments are shown ($n = 8$). Unpaired, two-tailed Student *t* tests were used to compare groups. * $p < 0.05$, ** $p < 0.01$, *** $p < 0.001$.

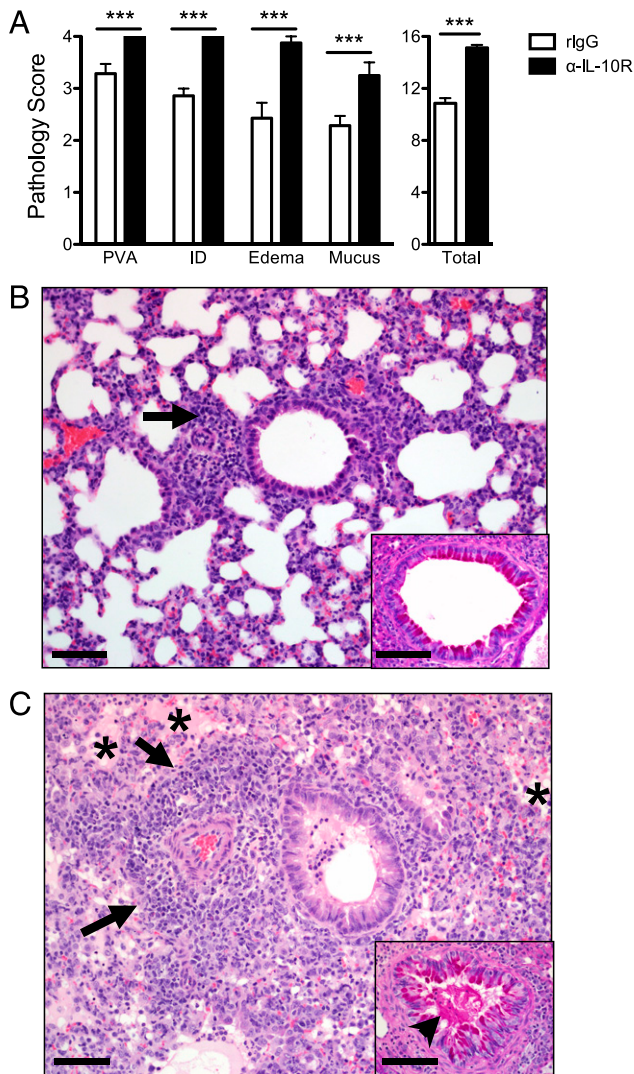


FIGURE 9. Increased lung pathology following IL-10R blockade. *A*, Cumulative pathological scoring analysis of sections from whole lungs of rIgG and anti-IL-10R mAb-treated mice following RSV infection. Representative H&E-stained images with PAS stain (*inset*; scale bar, 110 μ m) from rIgG- (*B*) and anti-IL-10R mAb-treated lungs (*C*). Scale bar, 75 μ m. Edema (asterisks), inflammation (arrows), and mucous cell proliferation with lumen obstruction (*inset*, arrowhead) can be seen. Cumulative data from two independent experiments are shown ($n = 8$). One-sample and two-sample t tests were used to compare groups. * $p < 0.05$, ** $p < 0.01$, *** $p < 0.001$.

associated with increased disease severity following RSV infection.

Alteration of additional CD4⁺ T cell subsets following IL-10R blockade

With the increased Th1 CD4⁺ T cell response during RSV infection in the absence of IL-10, we wanted to investigate the effect of IL-10 deficiency on additional CD4⁺ T cell subsets. IL-10R blockade resulted in alterations in the Treg and Th17 CD4⁺ T cell subsets following acute RSV infection (Fig. 10). To determine changes in the natural and inducible Treg compartments, we identified natural Tregs by their expression of the transcription factor Helios (35, 36). On day 8 p.i., a significant decrease occurs in Foxp3⁺Helios⁺ CD4⁺ T cells in the lung ($p < 0.01$), medLNs, ($p < 0.001$), and BAL ($p < 0.05$) in mice administered anti-IL-10R mAb (Fig. 10A). However, there is no difference between

mice treated with the anti-IL-10R mAb and controls in the total number of Foxp3⁺Helios⁻ CD4⁺ T cells. These data suggest that IL-10, directly or indirectly, supports the maintenance or induction of natural Tregs during an acute RSV infection.

Coincident with the decrease in the total number of natural Tregs, we observed a significant increase in the total number of IL-17A-producing CD4⁺ T cells in mice treated with anti-IL-10R mAb (Fig. 10B). On day 8 p.i., IL-17A⁺ CD4⁺ T cells are significantly increased following IL-10R blockade in the lung ($p < 0.01$) and BAL ($p < 0.05$) during acute RSV infection. Similar results were obtained using IL-10 KO mice (data not shown). We did not observe IL-17A-producing CD4⁺ T cells in the medLN or IL-17F-producing cells in the lung, medLNs, and BAL of experimental or control mice (data not shown). Thus, IL-10R blockade leads to decreased numbers of Tregs in the lung with a concomitant increase in the number of Th17 cells.

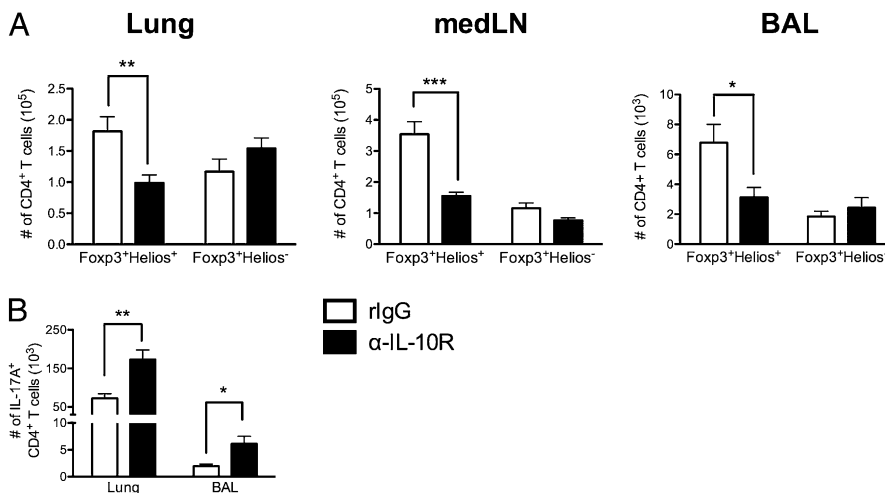
Discussion

In this article, we examined the kinetics of IL-10 production during acute RSV infection and found that the highest frequency of IL-10-producing cells occurred between days 6 through 10 p.i., a time frame that overlaps with the virus-specific adaptive immune response (Fig. 1; Supplemental Fig. 1) (37, 38). We found that three major subsets of CD4⁺ T cells were responsible for the majority of IL-10 production at the peak of the immune response following RSV infection (Fig. 3). Approximately one-third of the IL-10-producing CD4⁺ T cells expressed Foxp3, representing a portion of the Treg population, whereas the remainder were conventional Foxp3⁻ CD4⁺ T cells that produced either IL-10 alone or coproduced IFN- γ . In addition, we observed a small frequency of IL-10⁺ IFN- γ ⁺ regulatory (Foxp3⁺) CD4⁺ T cells only in the lung airways following RSV infection. We hypothesize that the environment in the lung airways is unique, causing these CD4⁺ T cells to alter their phenotype. We are currently investigating the plasticity of these IL-10⁺ IFN- γ ⁺ regulatory (Foxp3⁺) CD4⁺ T cells and their role during acute RSV infection.

Th1 cells have been previously reported to be the major producers of IL-10 in other pathogenic models, including influenza A virus (IAV), *Leishmania* species, mycobacterial, and *Borrelia burgdorferi* infections (39–43). The observation that other CD4⁺ T cell subsets are capable of producing IL-10, and that IL-10 can regulate T cell function, has led to the hypothesis that IL-10 acts in either an autocrine manner to directly suppress T cell activation or a paracrine manner through DCs to control immunopathology (11, 44–46). Our results support the conclusion that in the absence of IL-10 and its regulation of T cells, increased RSV-induced disease severity is a consequence of increased immunopathology. However, the molecular mechanisms that induce IL-10 production by effector T cells during RSV infection remain to be determined.

We demonstrate that CD4⁺ T cells produce the majority of IL-10 in vivo during an acute RSV infection. In contrast, we observe only a small number of IL-10-producing CD8⁺ T cells (Fig. 1). IL-10 production by T cells has been examined in a number of other respiratory virus infections. Consistent with our results, McKinstry et al. (43) recently reported that CD4⁺ T cells make the majority of IL-10 during a high-dose IAV infection. Virus-specific CD8⁺ T cells that coproduce IL-10 and IFN- γ in the lung have been reported during acute SV5 infection (47). However, these studies did not assess IL-10 production by CD4⁺ T cells during SV5 infection. Therefore it is unclear if either CD4⁺ or CD8⁺ T cells represent the dominant cell source of IL-10 during acute SV5 infection. In contrast to our findings with RSV, Sun et al. (48)

FIGURE 10. Increased Th17 response and decrease in Treg response following IL-10R blockade. A, At day 8 p.i., natural Tregs (Foxp3⁺Helios⁺) and inducible Tregs (Foxp3⁺Helios⁻) were quantified in the lung, medLN, and BAL of RSV-infected mice administered anti-IL-10R mAb. B, At day 8 p.i., Th17 cells were quantified by intracellular staining of IL-17A in the lung and BAL of anti-IL-10R mAb-treated mice infected with RSV. Cumulative data from two independent experiments are shown ($n = 8$). Unpaired, two-tailed Student *t* tests were used to compare groups. * $p < 0.05$, ** $p < 0.01$, *** $p < 0.001$.



report that CD8⁺ T cells are responsible for the majority of IL-10 production during an acute low-dose IAV infection. It is currently unclear what accounts for the reported discrepancies in the proportion of CD4⁺ and CD8⁺ T cells that make IL-10 during respiratory viral infections. A more recent study by Sun et al. (49) indicates that IL-10 production by CD8⁺ T cells during an acute IAV infection requires the expression of Blimp-1 and is synergistically promoted by IL-2 produced by helper CD4⁺ T cells as well as IL-27 produced by innate immune cells. It remains to be determined if the reduced number of IL-10-producing CD8⁺ T cells during an acute RSV infection is the result of a lack of CD4⁺ T cell help and/or decreased IL-27 production.

Exacerbated disease severity and increased levels of proinflammatory cytokines and chemokines were observed in the absence of IL-10 following RSV infection (Figs. 4, 6). However, we did not observe any changes in peak viral titers (day 4 p.i.) or viral clearance (day 7 p.i.) between IL-10 KO or anti-IL-10R mAb-treated mice compared with their controls (Fig. 5). These data support the idea that increased disease severity is independent of RSV replication and clearance kinetics (23). Instead, alterations in the RSV immune response (i.e., increased inflammatory conditions) result in increased immunopathology. Similarly, Haeberle et al. (50) reported that treatment with rIL-10 significantly decreased the production of chemokines, such as CCL2, CCL3, and CCL5, in the lung airways when analyzed 24 h after RSV infection. CCL5 has been positively associated with RSV-induced disease severity, and blocking CCL5 results in the increased production of IL-12 and decreased airway hyperreactivity (51). Consistent with its effect on chemokine production, treatment with rIL-10 significantly reduced the number of cellular infiltrating lymphocytes and decreased alveolar inflammation following acute RSV infection (50). Exogenous addition of IL-10 did not affect viral replication (50). We demonstrate that IL-10 deficiency significantly increases weight loss and airway resistance following RSV infection (Fig. 4). The above results combined with our findings suggest that IL-10 acts by inhibiting proinflammatory cytokine production in the lung, which in turn reduces RSV-induced pulmonary inflammation and immunopathology.

Similar to these observations, findings from the avian H5N1 outbreaks in Hong Kong revealed that patients with severe disease exhibited high serum cytokine levels of IL-6, TNF- α , and IFN- γ and increased serum chemokine levels of CCL2, CXCL9, and CXCL10 when compared with less severely ill controls (8, 52–55). The levels of IL-6, IFN- α , IFN- γ , CCL2, and CXCL10 were

also significantly elevated in the serum of SARS patients with more severe disease (56–58). Overall, in the absence of IL-10 our data support the notion that a strong proinflammatory response contributes to increased RSV disease severity. Thus therapeutic approaches aimed at increasing IL-10 production may offer a means to decrease RSV-induced immunopathology without affecting viral clearance.

IL-10R blockade resulted in an increase in the magnitude and effector function of RSV-specific CD8⁺ T cells and CD4⁺ T cells (Figs. 7, 8). A similar observation was reported by Sun et al. (48), in which acute IAV infection resulted in an increased total number of IFN- γ -producing CD8⁺ and CD4⁺ T cells in mice treated with anti-IL-10R mAb. In addition, we observed a significant rise in the number of Th17 CD4⁺ T cells during an acute RSV infection in the absence of IL-10 (Fig. 10). In agreement with our findings, McKinstry et al. (43) recently reported a significant increase in IL-17 production and the accumulation of Th17 cells in the lungs of IL-10 KO mice following an acute high-dose IAV infection.

In contrast to the increased number of Th17 cells discussed above, we observed a decrease in the total number of Helios⁺ Foxp3⁺ Tregs in the lung following IL-10R blockade in RSV-infected mice. Recent work suggests that Helios expression may selectively identify natural Tregs (35, 36). Thus, the decreased number of natural Tregs may directly contribute to increased disease severity. In recent studies, depletion of natural Tregs results in exacerbated RSV-induced disease and more IFN- γ ⁺ TNF- α ⁺ CD8⁺ T cells (29, 59). In a model of colitis, IL-10 was reported to be necessary to maintain Foxp3 expression of CD4⁺ T cells under inflammatory conditions (60). Murai et al. demonstrated that the suppressive function of Tregs was maintained by IL-10R expression and the capacity to directly respond to IL-10. However, the environment in the intestinal mucosa is unique, with different regulatory factors than those in the lung, and the findings of Murai et al. may not necessarily translate to lung mucosal tissue. Therefore, the role of IL-10 in the regulation of Foxp3 expression will need to be further evaluated in the lung environment. We are currently examining the role of IL-10 in the induction and/or maintenance of pulmonary Tregs during acute RSV infection.

IL-10 polymorphisms have been associated with RSV-induced disease severity in humans (61, 62). In this article, we demonstrate that IL-10 plays a critical role in regulating the immune response and preventing exacerbated disease due to immune-mediated pulmonary injury during acute RSV infection. Multiple

respiratory viruses, such as pandemic IAV strains and the human coronavirus that causes SARS, are believed to induce immunopathology resulting in severe morbidity and mortality (8, 9, 56–58). Therefore, identifying novel approaches to modulate virus-induced immunopathology would be beneficial in treating acute respiratory viral infections. Exogenous IL-10 treatment has been shown to be safe and well tolerated in clinical trials for several chronic inflammatory diseases, including Crohn's disease, psoriasis, and chronic hepatitis C (63–68). In patients with chronic hepatitis C who were nonresponsive to IFN-based therapy, IL-10 treatment did not affect viral titers but reduced chronic liver inflammation and fibrosis (66). Using IL-10 as an immunosuppressive treatment during a respiratory viral infection resulting in immunopathology may be feasible to prevent severe morbidity and mortality. Our data indicate that IL-10 is an attractive target based on its ability to regulate RSV-induced innate and adaptive immune responses without affecting viral clearance.

Acknowledgments

We thank Drs. John Harty and Stanley Perlman for critical review of the manuscript and Stacey Hartwig for excellent technical assistance.

Disclosures

The authors have no financial conflicts of interest.

References

- Falsey, A. R., P. A. Hennessey, M. A. Formica, C. Cox, and E. E. Walsh. 2005. Respiratory syncytial virus infection in elderly and high-risk adults. *N. Engl. J. Med.* 352: 1749–1759.
- Falsey, A. R., and E. E. Walsh. 2005. Respiratory syncytial virus infection in elderly adults. *Drugs Aging* 22: 577–587.
- Heilman, C. A. 1990. From the National Institute of Allergy and Infectious Diseases and the World Health Organization. Respiratory syncytial and parainfluenza viruses. *J. Infect. Dis.* 161: 402–406.
- Ebbert, J. O., and A. H. Limper. 2005. Respiratory syncytial virus pneumonitis in immunocompromised adults: clinical features and outcome. *Respiration* 72: 263–269.
- Shay, D. K., R. C. Holman, R. D. Newman, L. L. Liu, J. W. Stout, and L. J. Anderson. 1999. Bronchiolitis-associated hospitalizations among US children, 1980–1996. *JAMA* 282: 1440–1446.
- Shay, D. K., R. C. Holman, G. E. Roosevelt, M. J. Clarke, and L. J. Anderson. 2001. Bronchiolitis-associated mortality and estimates of respiratory syncytial virus-associated deaths among US children, 1979–1997. *J. Infect. Dis.* 183: 16–22.
- Collins, P. L., and B. S. Graham. 2008. Viral and host factors in human respiratory syncytial virus pathogenesis. *J. Virol.* 82: 2040–2055.
- La Gruta, N. L., K. Kedzierska, J. Stambas, and P. C. Doherty. 2007. A question of self-preservation: immunopathology in influenza virus infection. *Immunol. Cell Biol.* 85: 85–92.
- Perlman, S., and A. A. Dandekar. 2005. Immunopathogenesis of coronavirus infections: implications for SARS. *Nat. Rev. Immunol.* 5: 917–927.
- Holt, P. G., D. H. Strickland, M. E. Wikström, and F. L. Jahnsen. 2008. Regulation of immunological homeostasis in the respiratory tract. *Nat. Rev. Immunol.* 8: 142–152.
- Saraiva, M., and A. O'Garra. 2010. The regulation of IL-10 production by immune cells. *Nat. Rev. Immunol.* 10: 170–181.
- Kotenko, S. V., C. D. Krause, L. S. Izotova, B. P. Pollack, W. Wu, and S. Pestka. 1997. Identification and functional characterization of a second chain of the interleukin-10 receptor complex. *EMBO J.* 16: 5894–5903.
- Liu, Y., S. H. Wei, A. S. Ho, R. de Waal Malefyt, and K. W. Moore. 1994. Expression cloning and characterization of a human IL-10 receptor. *J. Immunol.* 152: 1821–1829.
- Tan, J. C., S. R. Indelicato, S. K. Narula, P. J. Zavodny, and C. C. Chou. 1993. Characterization of interleukin-10 receptors on human and mouse cells. *J. Biol. Chem.* 268: 21053–21059.
- Moore, K. W., R. de Waal Malefyt, R. L. Coffman, and A. O'Garra. 2001. Interleukin-10 and the interleukin-10 receptor. *Annu. Rev. Immunol.* 19: 683–765.
- de Waal Malefyt, R., J. Haanen, E. Spits, M. G. Roncarolo, A. te Velde, C. Figdor, K. Johnson, R. Kastelein, H. Yssel, and J. E. de Vries. 1991. Interleukin 10 (IL-10) and viral IL-10 strongly reduce antigen-specific human T cell proliferation by diminishing the antigen-presenting capacity of monocytes via downregulation of class II major histocompatibility complex expression. *J. Exp. Med.* 174: 915–924.
- Ding, L., P. S. Linsley, L. Y. Huang, R. N. Germain, and E. M. Shevach. 1993. IL-10 inhibits macrophage costimulatory activity by selectively inhibiting the up-regulation of B7 expression. *J. Immunol.* 151: 1224–1234.
- Allavena, P., L. Piemonti, D. Longoni, S. Bernasconi, A. Stoppacciaro, L. Ruco, and A. Mantovani. 1998. IL-10 prevents the differentiation of monocytes to dendritic cells but promotes their maturation to macrophages. *Eur. J. Immunol.* 28: 359–369.
- Schandené, L., C. Alonso-Vega, F. Willems, C. Gérard, A. Delvaux, T. Velu, R. Devos, M. de Boer, and M. Goldman. 1994. B7/CD28-dependent IL-5 production by human resting T cells is inhibited by IL-10. *J. Immunol.* 152: 4368–4374.
- Taga, K., H. Mostowski, and G. Tosato. 1993. Human interleukin-10 can directly inhibit T-cell growth. *Blood* 81: 2964–2971.
- de Waal Malefyt, R., H. Yssel, and J. E. de Vries. 1993. Direct effects of IL-10 on subsets of human CD4⁺ T cell clones and resting T cells. Specific inhibition of IL-2 production and proliferation. *J. Immunol.* 150: 4754–4765.
- Couper, K. N., D. G. Blount, and E. M. Riley. 2008. IL-10: the master regulator of immunity to infection. *J. Immunol.* 180: 5771–5777.
- Graham, B. S., L. A. Bunton, P. F. Wright, and D. T. Karzon. 1991. Role of T lymphocyte subsets in the pathogenesis of primary infection and rechallenge with respiratory syncytial virus in mice. *J. Clin. Invest.* 88: 1026–1033.
- Peebles, R. S., Jr., and B. S. Graham. 2005. Pathogenesis of respiratory syncytial virus infection in the murine model. *Proc. Am. Thorac. Soc.* 2: 110–115.
- Berg, D. J., N. Davidson, R. Kühn, W. Müller, S. Menon, G. Holland, L. Thompson-Snipes, M. W. Leach, and D. Rennick. 1996. Enterocolitis and colon cancer in interleukin-10-deficient mice are associated with aberrant cytokine production and CD4⁺ T_H1-like responses. *J. Clin. Invest.* 98: 1010–1020.
- Kühn, R., J. Löhler, D. Rennick, K. Rajewsky, and W. Müller. 1993. Interleukin-10-deficient mice develop chronic enterocolitis. *Cell* 75: 263–274.
- Madan, R., F. Demircik, S. Surianarayanan, J. L. Allen, S. Divanovic, A. Trompette, N. Yogeve, Y. Gu, M. Khoudoun, D. Hildeman, et al. 2009. Non-redundant roles for B cell-derived IL-10 in immune counter-regulation. *J. Immunol.* 183: 2312–2320.
- Castilow, E. M., K. L. Legge, and S. M. Varga. 2008. Cutting edge: Eosinophils do not contribute to respiratory syncytial virus vaccine-enhanced disease. *J. Immunol.* 181: 6692–6696.
- Fulton, R. B., D. K. Meyerholz, and S. M. Varga. 2010. Foxp3⁺ CD4 regulatory T cells limit pulmonary immunopathology by modulating the CD8 T cell response during respiratory syncytial virus infection. *J. Immunol.* 185: 2382–2392.
- Hamelmann, E., J. Schwarze, K. Takeda, A. Oshiba, G. L. Larsen, C. G. Irvin, and E. W. Gelfand. 1997. Noninvasive measurement of airway responsiveness in allergic mice using barometric plethysmography. *Am. J. Respir. Crit. Care Med.* 156: 766–775.
- Fulton, R. B., M. R. Olson, and S. M. Varga. 2008. Regulation of cytokine production by virus-specific CD8 T cells in the lungs. *J. Virol.* 82: 7799–7811.
- Olson, M. R., S. M. Hartwig, and S. M. Varga. 2008. The number of respiratory syncytial virus (RSV)-specific memory CD8 T cells in the lung is critical for their ability to inhibit RSV vaccine-enhanced pulmonary eosinophilia. *J. Immunol.* 181: 7958–7968.
- Castilow, E. M., D. K. Meyerholz, and S. M. Varga. 2008. IL-13 is required for eosinophil entry into the lung during respiratory syncytial virus vaccine-enhanced disease. *J. Immunol.* 180: 2376–2384.
- Rai, D., N. L. Pham, J. T. Harty, and V. P. Badovinac. 2009. Tracking the total CD8 T cell response to infection reveals substantial discordance in magnitude and kinetics between inbred and outbred hosts. *J. Immunol.* 183: 7672–7681.
- Sugimoto, N., T. Oida, K. Hirota, K. Nakamura, T. Nomura, T. Uchiyama, and S. Sakaguchi. 2006. Foxp3-dependent and -independent molecules specific for CD25⁺CD4⁺ natural regulatory T cells revealed by DNA microarray analysis. *Int. Immunol.* 18: 1197–1209.
- Thornton, A. M., P. E. Korty, D. Q. Tran, E. A. Wohlfert, P. E. Murray, Y. Belkaid, and E. M. Shevach. 2010. Expression of Helios, an Ikaros transcription factor family member, differentiates thymic-derived from peripherally induced Foxp3⁺ T regulatory cells. *J. Immunol.* 184: 3433–3441.
- Chang, J., and T. J. Braciale. 2002. Respiratory syncytial virus infection suppresses lung CD8⁺ T-cell effector activity and peripheral CD8⁺ T-cell memory in the respiratory tract. *Nat. Med.* 8: 54–60.
- Chang, J., A. Srikiatkachorn, and T. J. Braciale. 2001. Visualization and characterization of respiratory syncytial virus F-specific CD8⁺ T cells during experimental virus infection. *J. Immunol.* 167: 4254–4260.
- Anderson, C. F., M. Oukka, V. J. Kuchroo, and D. Sacks. 2007. CD4⁺CD25⁺ Foxp3⁺ Th1 cells are the source of IL-10-mediated immune suppression in chronic cutaneous leishmaniasis. *J. Exp. Med.* 204: 285–297.
- Gerosa, F., C. Nisii, S. Righetti, R. Micciolo, M. Marchesini, A. Cazzadori, and G. Trinchieri. 1999. CD4⁺ T cell clones producing both interferon-gamma and interleukin-10 predominate in bronchoalveolar lavages of active pulmonary tuberculosis patients. *Clin. Immunol.* 92: 224–234.
- Jankovic, D., M. C. Kullberg, C. G. Feng, R. S. Goldszmid, C. M. Collazo, M. Wilson, T. A. Wynn, M. Kamanaka, R. A. Flavell, and A. Sher. 2007. Conventional T-bet⁺Foxp3⁺ Th1 cells are the major source of host-protective regulatory IL-10 during intracellular protozoan infection. *J. Exp. Med.* 204: 273–283.
- Pohl-Koppe, A., K. E. Balashov, A. C. Steere, E. L. Logigian, and D. A. Hafler. 1998. Identification of a T cell subset capable of both IFN- γ and IL-10 secretion in patients with chronic *Borrelia burgdorferi* infection. *J. Immunol.* 160: 1804–1810.

43. McKinstry, K. K., T. M. Strutt, A. Buck, J. D. Curtis, J. P. Dibble, G. Huston, M. Tighe, H. Hamada, S. Sell, R. W. Dutton, and S. L. Swain. 2009. IL-10 deficiency unleashes an influenza-specific Th17 response and enhances survival against high-dose challenge. *J. Immunol.* 182: 7353–7363.
44. Maynard, C. L., and C. T. Weaver. 2008. Diversity in the contribution of interleukin-10 to T-cell-mediated immune regulation. *Immunol. Rev.* 226: 219–233.
45. O'Garra, A., and P. Vieira. 2007. Th1 cells control themselves by producing interleukin-10. *Nat. Rev. Immunol.* 7: 425–428.
46. Shaw, M. H., G. J. Freeman, M. F. Scott, B. A. Fox, D. J. Bzik, Y. Belkaid, and G. S. Yap. 2006. Tyk2 negatively regulates adaptive Th1 immunity by mediating IL-10 signaling and promoting IFN-gamma-dependent IL-10 reactivation. *J. Immunol.* 176: 7263–7271.
47. Palmer, E. M., B. C. Holbrook, S. Arimilli, G. D. Parks, and M. A. Alexander-Miller. 2010. IFN-gamma-producing, virus-specific CD8⁺ effector cells acquire the ability to produce IL-10 as a result of entry into the infected lung environment. *Virology* 404: 225–230.
48. Sun, J., R. Madan, C. L. Karp, and T. J. Braciale. 2009. Effector T cells control lung inflammation during acute influenza virus infection by producing IL-10. *Nat. Med.* 15: 277–284.
49. Sun, J., H. Dodd, E. K. Moser, R. Sharma, and T. J. Braciale. 2011. CD4⁺ T cell help and innate-derived IL-27 induce Blimp-1-dependent IL-10 production by antiviral CTLs. *Nat. Immunol.* 12: 327–334.
50. Haeberle, H. A., A. Casola, Z. Gatalica, S. Petronella, H. J. Dieterich, P. B. Ernst, A. R. Brasier, and R. P. Garofalo. 2004. IκappaB kinase is a critical regulator of chemokine expression and lung inflammation in respiratory syncytial virus infection. *J. Virol.* 78: 2232–2241.
51. Tekkanat, K. K., H. Maassab, A. Miller, A. A. Berlin, S. L. Kunkel, and N. W. Lukacs. 2002. RANTES (CCL5) production during primary respiratory syncytial virus infection exacerbates airway disease. *Eur. J. Immunol.* 32: 3276–3284.
52. de Jong, M. D., C. P. Simmons, T. T. Thanh, V. M. Hien, G. J. Smith, T. N. Chau, D. M. Hoang, N. V. Chau, T. H. Khanh, V. C. Dong, et al. 2006. Fatal outcome of human influenza A (H5N1) is associated with high viral load and hypercytokinemia. *Nat. Med.* 12: 1203–1207.
53. Peiris, J. S., W. C. Yu, C. W. Leung, C. Y. Cheung, W. F. Ng, J. M. Nicholls, T. K. Ng, K. H. Chan, S. T. Lai, W. L. Lim, et al. 2004. Re-emergence of fatal human influenza A subtype H5N1 disease. *Lancet* 363: 617–619.
54. To, K. F., P. K. Chan, K. F. Chan, W. K. Lee, W. Y. Lam, K. F. Wong, N. L. Tang, D. N. Tsang, R. Y. Sung, T. A. Buckley, et al. 2001. Pathology of fatal human influenza associated with avian influenza A H5N1 virus. *J. Med. Virol.* 63: 242–246.
55. Beigel, J. H., J. Farrar, A. M. Han, F. G. Hayden, R. Hyer, M. D. de Jong, S. Lochindarat, T. K. Nguyen, T. H. Nguyen, T. H. Tran, et al; Writing Committee of the World Health Organization (WHO) Consultation on Human Influenza A/H5. 2005. Avian influenza A (H5N1) infection in humans. *N. Engl. J. Med.* 353: 1374–1385.
56. Cameron, M. J., L. Ran, L. Xu, A. Danesh, J. F. Bermejo-Martin, C. M. Cameron, M. P. Muller, W. L. Gold, S. E. Richardson, S. M. Poutanen, et al; Canadian SARS Research Network. 2007. Interferon-mediated immunopathological events are associated with atypical innate and adaptive immune responses in patients with severe acute respiratory syndrome. *J. Virol.* 81: 8692–8706.
57. Wong, C. K., C. W. Lam, A. K. Wu, W. K. Ip, N. L. Lee, I. H. Chan, L. C. Lit, D. S. Hui, M. H. Chan, S. S. Chung, and J. J. Sung. 2004. Plasma inflammatory cytokines and chemokines in severe acute respiratory syndrome. *Clin. Exp. Immunol.* 136: 95–103.
58. Zhang, Y., J. Li, Y. Zhan, L. Wu, X. Yu, W. Zhang, L. Ye, S. Xu, R. Sun, Y. Wang, and J. Lou. 2004. Analysis of serum cytokines in patients with severe acute respiratory syndrome. *Infect. Immun.* 72: 4410–4415.
59. Lee, D. C., J. A. Harker, J. S. Tregoning, S. F. Atabani, C. Johansson, J. Schwarze, and P. J. Openshaw. 2010. CD25⁺ natural regulatory T cells are critical in limiting innate and adaptive immunity and resolving disease following respiratory syncytial virus infection. *J. Virol.* 84: 8790–8798.
60. Murai, M., O. Turovskaya, G. Kim, R. Madan, C. L. Karp, H. Cheroutre, and M. Kronenberg. 2009. Interleukin 10 acts on regulatory T cells to maintain expression of the transcription factor Foxp3 and suppressive function in mice with colitis. *Nat. Immunol.* 10: 1178–1184.
61. Wilson, J., K. Rowlands, K. Rockett, C. Moore, E. Lockhart, M. Sharland, D. Kwiatkowski, and J. Hull. 2005. Genetic variation at the IL10 gene locus is associated with severity of respiratory syncytial virus bronchiolitis. *J. Infect. Dis.* 191: 1705–1709.
62. Hoebee, B., L. Bont, E. Rietveld, M. van Oosten, H. M. Hodemaekers, N. J. Nagelkerke, H. J. Neijens, J. L. Kimpfen, and T. G. Kimman. 2004. Influence of promoter variants of interleukin-10, interleukin-9, and tumor necrosis factor-alpha genes on respiratory syncytial virus bronchiolitis. *J. Infect. Dis.* 189: 239–247.
63. Asadullah, K., W. D. Döcke, M. Ebeling, M. Friedrich, G. Belbe, H. Audring, H. D. Volk, and W. Sterry. 1999. Interleukin 10 treatment of psoriasis: clinical results of a phase 2 trial. *Arch. Dermatol.* 135: 187–192.
64. Braat, H., P. Rottiers, D. W. Hommes, N. Huyghebaert, E. Remaut, J. P. Remon, S. J. van Deventer, S. Neiryneck, M. P. Peppelenbosch, and L. Steidler. 2006. A phase I trial with transgenic bacteria expressing interleukin-10 in Crohn's disease. *Clin. Gastroenterol. Hepatol.* 4: 754–759.
65. Fedorak, R. N., A. Gangl, C. O. Elson, P. Rutgeerts, S. Schreiber, G. Wild, S. B. Hanauer, A. Kilian, M. Cohard, A. LeBeaut, and B. Feagan. 2000. Recombinant human interleukin 10 in the treatment of patients with mild to moderately active Crohn's disease. The Interleukin 10 Inflammatory Bowel Disease Cooperative Study Group. *Gastroenterology* 119: 1473–1482.
66. Nelson, D. R., G. Y. Lauwers, J. Y. Lau, and G. L. Davis. 2000. Interleukin 10 treatment reduces fibrosis in patients with chronic hepatitis C: a pilot trial of interferon nonresponders. *Gastroenterology* 118: 655–660.
67. Opal, S. M., J. C. Wherry, and P. Grint. 1998. Interleukin-10: potential benefits and possible risks in clinical infectious diseases. *Clin. Infect. Dis.* 27: 1497–1507.
68. Schreiber, S., R. N. Fedorak, O. H. Nielsen, G. Wild, C. N. Williams, S. Nikolaus, M. Jacyna, B. A. Lashner, A. Gangl, P. Rutgeerts, et al. 2000. Safety and efficacy of recombinant human interleukin 10 in chronic active Crohn's disease. Crohn's Disease IL-10 Cooperative Study Group. *Gastroenterology* 119: 1461–1472.

Supplemental Figure Legend

Figure S1. CD4⁺ T cells represent the majority of IL-10-producing cells at the peak of RSV infection. IL-10-eGFP C57BL/6 reporter mice were used to assess *in vivo* IL-10 production at the indicated time points following RSV infection. Lung and BAL cells were collected for analysis of IL-10-eGFP expression by flow cytometry (left panels). Anti-Thy1.2 Ab staining was used to determine the frequency of T cells within the IL-10-producing cell population (middle panels). IL-10-producing T cells were further gated on CD4 and CD8 to determine the distribution of IL-10-producing T cells (right panels). Numbers indicate the frequency of the gated cells. Plots are concatenated using Flowjo software showing equal representation of three individual mice at each time point. Data are representative of three independent experiments ($n = 9$).

Supplemental Figure 1

